

Combining Ordered Subsets and Momentum for Accelerated X-ray CT Image Reconstruction: Supplementary material

Donghwan Kim, *Student Member, IEEE*, Sathish Ramani, *Member, IEEE*, and Jeffrey A. Fessler, *Fellow, IEEE*

Abstract—This material extends the result section of [1] by illustrating the proposed OS-momentum algorithms using abdominal region CT scan data. These additional results confirm the dramatic acceleration provided by OS-momentum methods. This material also provides a table of notation for [1].

References to equations, tables, figures, bibliography are within this material unless specified otherwise.

I. ABDOMINAL REGION SCAN

We reconstructed a $600 \times 600 \times 222$ abdominal region image (in Fig. 1) from $888 \times 64 \times 3611$ sinogram data measured in a helical geometry with pitch 1.0. We measured the RMSD of the proposed OS-momentum algorithms for 24 and 48 subsets using bit-reversal ordering (OSb) in OS methods. The convergence results in Fig. 2(a) are similar to that of two data sets in [1], where $\lambda = 0.01$ is more effective than $\lambda = 0.1$ for stabilizing OS-momentum. However, the case $M = 48$ accumulated more gradient error than two other data sets in [1], particularly the un-relaxed ($\lambda = 0$) OS-momentum for $M = 48$ becomes very unstable. So the choice $\lambda = 0.01$ was not large enough to suppress the large accumulating error in first 10 iterations than $\lambda = 0.1$.

Fig. 2(b) shows the results using the oracle $\hat{u}_j = |x_j^{(0)} - \hat{x}_j|$ in [1, eqn. (26)] for 48 subsets, compared to those using the approximate $\zeta \bar{u}$ [1, eqn. (29)] of \hat{u} . The oracle parameter \hat{u} worked well for both $\lambda = 0.1$ and 0.01 , indicating that the convergence rate depends less on λ when the voxel-dependent factor $\zeta \bar{u}_j$ better approximates \hat{u}_j , and we leave this as future work.

Fig. 1 shows the initial FBP image, converged image, and the reconstructed image at 15th iteration from the proposed algorithm. The reconstructed image is very close to the converged image after 15 iterations, largely removing the streak artifacts in FBP.

II. TABLE OF NOTATIONS

Table I illustrates notations used in [1].

Date of current version August 19, 2014. This work was supported in part by GE Healthcare, the National Institutes of Health under Grant R01-HL-098686, and equipment donations from Intel Corporation.

Donghwan Kim is with the Department of Electrical Engineering and Computer Science, University of Michigan, Ann Arbor, MI 48105 USA (e-mail: kimdongh@umich.edu).

Sathish Ramani is with the GE Global Research Center, Niskayuna, NY 12309 USA (e-mail: umrsat@gmail.com).

Jeffrey A. Fessler is with the Department of Electrical Engineering and Computer Science, University of Michigan, Ann Arbor, MI 48105 USA (e-mail: fessler@umich.edu).

TABLE I
TABLE OF NOTATIONS IN [1]

System			
\mathbf{y}	Measured data	\mathbf{A}	System matrix
\mathbf{x}	Image	ϵ	Noise
PWLS cost function			
$\Psi(\mathbf{x})$	Cost function	$\hat{\mathbf{x}}$	The minimizer
\mathcal{X}	Feasible region of image \mathbf{x}	\mathbf{W}	Ray-dependent weighting matrix
$R(\mathbf{x})$	Regularization function	C	Finite-difference matrix
$\psi_r(t)$	Edge-preserving potential function	β_r	Spatial weighting coefficient
Optimization			
$\phi(\mathbf{x}; \mathbf{x}^{(n)})$	Surrogate function	\mathbf{D}	Diagonal majorizing matrix
$\mathcal{P}_{\mathcal{X}}[\mathbf{x}]$	Projection of \mathbf{x} onto \mathcal{X}	n	Iteration counter
M	Number of subsets	m	Subset index
$\Psi_m(\mathbf{x})$	Subset-based cost function	k	Subiteration counter
t_k	Momentum coefficient	\mathbf{v}, \mathbf{z}	Auxiliary image spaces
Stochastic gradient			
S_k	Random variable of subset index	ξ_k	Realization of S_k
\mathcal{B}	Bounded feasible region of \mathbf{x}	\mathbf{p}	Voxel-wise diameter of \mathcal{B}
σ	Stochastic error bound	$\tilde{\sigma}(\mathbf{x})$	Stochastic error bound for given \mathbf{x}
Relaxation			
$\Gamma^{(k)}$	Relaxed diagonal majorizing matrix	Γ	Diagonal matrix for $\Gamma^{(k)}$ update
c_k	Coefficient for $\Gamma^{(k)}$ update	η	Coefficient for c_k update
α_k	Coefficient for t_k update	$\hat{\mathbf{D}}$	\mathbf{D} with nonuniform approach
$\hat{\mathbf{u}}$	Voxel-wise distance between $\mathbf{x}^{(0)}$ and $\hat{\mathbf{x}}$	$\bar{\mathbf{u}}$	Normalized approximation of $\hat{\mathbf{u}}$
ζ	Coefficient for approximating $\hat{\mathbf{u}}$	λ	Coefficient for adjusting Γ

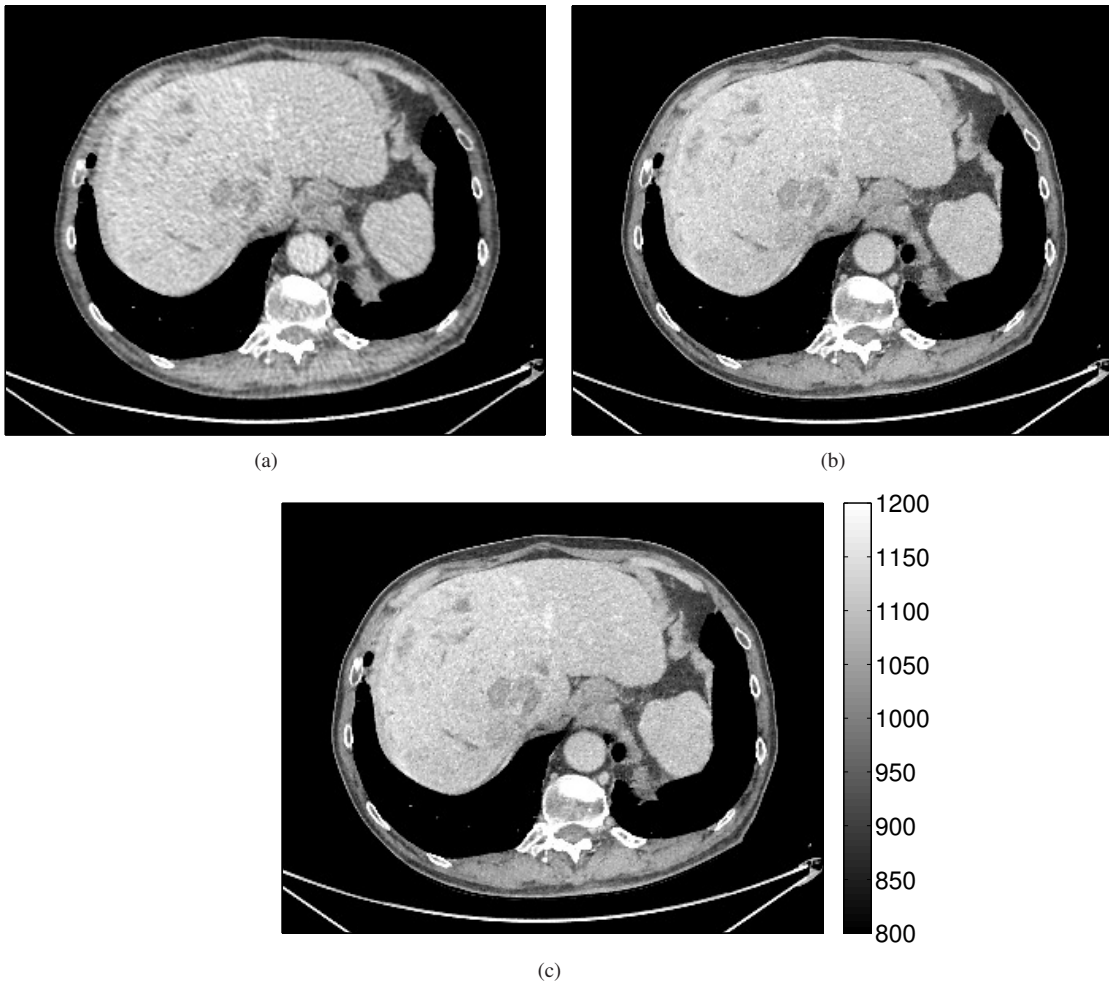


Fig. 1. Abdominal region scan: a transaxial plane of (a) an initial FBP image $\mathbf{x}^{(0)}$, (b) a converged image $\hat{\mathbf{x}}$, and (c) an image $\mathbf{x}^{(15)}$ after 15 iterations (about 1220 seconds) of OSb(24)-mom3 where $(c, \zeta, \lambda) = (1.5, 30, 0.01)$. (Images are cropped for better visualization.)

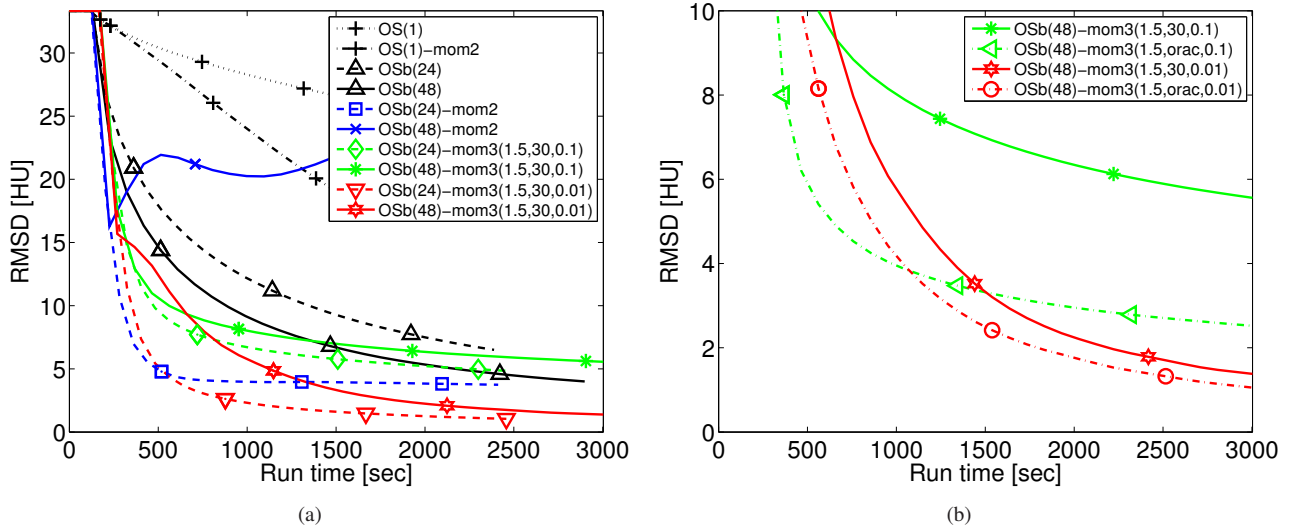


Fig. 2. Abdominal region scan: convergence rate of OSb methods (24, 48 subsets) for 30 iterations with and without momentum for several choices of (c, ζ, λ) with (a) the choice $\zeta \hat{u} (\approx \hat{u})$ in [1, eqn. (29)] with $\zeta = 30$ [HU] and (b) the oracle choice \hat{u} [1, eqn. (26)] for 48 subsets.

REFERENCES

[1] D. Kim, S. Ramani, and J. A. Fessler, "Combining ordered subsets and momentum for accelerated X-ray CT image reconstruction," *IEEE Trans. Med. Imag.*, 2014, Submitted.